



# MID-AMERICA TRANSPORTATION CENTER

Report # MATC-UNL: 004-44

Final Report

WBS: 27-1121-0005-004-44



## Bio-Inspired Reusable Crash Cushions with Superior Energy-Absorbing Capacity

**Congrui Grace Jin, PhD**

Assistant Professor  
Department of Civil and Environmental Engineering  
University of Nebraska-Lincoln

**Joshua Steelman, PhD**

Associate Professor

**Arman Moussavi, BS**

Master's Student



2024

A Cooperative Research Project sponsored by U.S. Department of Transportation- Office of the Assistant Secretary for Research and Technology

The contents of this report reflect the views of the authors, who are responsible for the facts and the accuracy of the information presented herein. This document is disseminated in the interest of information exchange. The report is funded, partially or entirely, by a grant from the U.S. Department of Transportation's University Transportation Centers Program. However, the U.S. Government assumes no liability for the contents or use thereof.

MATC

# Bio-Inspired Reusable Crash Cushions with Superior Energy-Absorbing Capacity

Congrui Grace Jin, Ph.D.  
Assistant Professor  
Department of Civil and Environmental Engineering  
University of Nebraska-Lincoln

Joshua Steelman, Ph.D.  
Associate Professor  
Department of Civil and Environmental Engineering  
University of Nebraska-Lincoln

Arman Moussavi, B.S.  
Master Student  
Department of Civil and Environmental Engineering  
University of Nebraska-Lincoln

A Report on Research Sponsored by

Mid-America Transportation Center

University of Nebraska–Lincoln

September 2024

## Technical Report Documentation Page

1. Report No. 25-1121-0005-051	2. Government Accession No.	3. Recipient's Catalog No.	
4. Title and Subtitle Bio-Inspired Reusable Crash Cushions with Superior Energy-Absorbing Capacity		5. Report Date September 2024	
		6. Performing Organization Code	
7. Author(s) Congrui Jin <a href="https://orcid.org/0000-0003-0606-5318">https://orcid.org/0000-0003-0606-5318</a> Arman Moussavi <a href="https://orcid.org/0009-0005-4361-4963">https://orcid.org/0009-0005-4361-4963</a>		8. Performing Organization Report No. 25-1121-0005-051	
9. Performing Organization Name and Address Mid-America Transportation Center Prem S. Paul Research Center at Whittier School 2200 Vine St. Lincoln, NE 68583-0851		10. Work Unit No. (TRAIS)	
		11. Contract or Grant No.	
12. Sponsoring Agency Name and Address Office of the Assistant Secretary for Research and Technology 1200 New Jersey Ave., SE Washington, D.C. 20590		13. Type of Report and Period Covered 09/01/2020 – 08/31/2022	
		14. Sponsoring Agency Code MATC TRB RiP No. 34760	
15. Supplementary Notes			
16. Abstract Roadside safety hardware, such as longitudinal barriers and crash cushions, is part of the highway infrastructure that is used to protect an errant vehicle from crashing into fixed roadside objects in a well-controlled manner. Despite constantly improved design and standardized full-scale impact testing of the roadside safety hardware, more than 3% of U.S. traffic fatalities are caused by the inefficiency of the roadside safety hardware. Innovative designs are urgently needed to improve the level of safety and decrease the severity of accidents. In nature, many plants and animals are optimized to adapt to various overload conditions and have demonstrated superior impact-resistant and energy-absorbing capabilities. Careful examination of these biological structures may inspire a new generation of roadside safety structural designs. This project comprehensively reviews the structure-property-performance relationship of the exemplary biological materials and demonstrate that the strategies used by the various biological role models can be understood, abstracted, modified, and transferred to bio-inspired roadside safety hardware.			
17. Key Words Roadside Safety Hardware; Longitudinal Barrier; Crash Cushion; Energy Dissipation; Impact Resistance; Bio-Inspired Design		18. Distribution Statement	
19. Security Classif. (of this report) Unclassified	20. Security Classif. (of this page) Unclassified	21. No. of Pages 38	22. Price

## Table of Contents

Disclaimer .....	v
Abstract .....	vi
Chapter 1 Introduction .....	1
Chapter 2 State of the Art of Roadside Hardware Design .....	3
2.1 Longitudinal Barrier.....	3
2.1.1 Types and Components of Longitudinal Barrier.....	3
2.1.2 Examples of Longitudinal Barrier.....	6
2.2 Crash Cushion.....	9
2.2.1 Types of Crash Cushion.....	9
2.2.2 Examples of Crash Cushion.....	13
2.3 Current Issues and Challenges .....	15
2.3.1 Issues for Motorcycles .....	16
2.3.2 Issues for Electric Vehicles.....	18
Chapter 3 Biology as Inspiration for the Design of Crash Cushions .....	22
3.1 Exemplary Biological Materials .....	22
3.1.1 Tree Bark.....	22
3.1.2 Coconut Endocarp.....	25
3.1.3 Sea Urchin Spines .....	29
3.1.4 Bovid Horn.....	31
Chapter 4 Concluding Remarks .....	34
References.....	35

## List of Figures

Figure 2.1 Schematic illustration of a terminal, a transition, a roadside barrier, a median barrier, and a bridge railing. This figure is not drawn to scale and for demonstrative purposes only.	4
Figure 2.2 Examples of longitudinal barrier include (a) MashFlex [9], (b) Sentry [10] (c) REBLOC [11], (d) SKT-SP [12], and (e) NETC Massachusetts Transition [13].	7
Figure 2.3 Schematic illustration of (a) a gating system, (b) a non-gating system, (c) a redirective system, and (d) a non-redirective system. A hazard is a roadside feature or object that can cause physical or economic harm or loss if reached by an errant vehicle.	12
Figure 2.4 Examples of crash cushion include (a) ENERGITE III [15], (b) RAPTOR [16], (c) EASI-CELL [17], (d) HEART (The picture is from Google Street View), (e) Universal TAU II [18], and (f) ADIEM [19].	15
Figure 3.1 (a) <i>S. giganteum</i> in Sequoia National Park, California, USA. (b) The tree bark of <i>S. giganteum</i> , consisting of a thin inner bark (IB) enclosed by a thick outer bark (OB). (c) $\mu$ CT of the cross-section of the outer bark. (d) A cross-section of the inner bark. (e) An enlarged view of the cross-section of the inner bark. (f) A cross-section of the outer bark. (g) A radial section of the outer bark. (h) Images from a typical drop-weight test of the <i>S. giganteum</i> bark. Modified and reproduced with permission [35]. Copyright 2020, MDPI.	24
Figure 3.2 The hierarchical composition of the coconut endocarp occurs on a total of eight hierarchical levels, denoted as H0 to H7. (a) A coconut fruit cut in half. (b) A coconut endocarp sample. (c) The cross-section of a vascular bundle in the sclereid cell matrix. (d) The sclereid cell matrix. (e) The cross-section of a fractured endocarp sample tested in compression. (f) A deflected crack in the sclereid cell matrix. (g) A deflected crack in a single sclereid cell. Modified and reproduced with permission [36]. Copyright 2020, MDPI.	28
Figure 3.3 (a) Photographs of the studied sea urchin species: <i>Heterocentrotus mammillatus</i> on the left and <i>Phyllacanthus imperialis</i> on the right. (b) Microphotographs of <i>Heterocentrotus mammillatus</i> spine cross sections. (c) Microphotographs of <i>Phyllacanthus imperialis</i> spine cross sections. (d) SE-mode SEM images of <i>Heterocentrotus mammillatus</i> and <i>Phyllacanthus imperialis</i> stereom structures. (e) Microphotographs showing characteristic stages of the fracture behavior of sea urchin spines under bulk compression. Modified and reproduced with permission [38]. Copyright 2009, Elsevier.	30
Figure 3.4 (a) Schematic view of the bovine horn and sampling positions. (b) SEM photograph of the cancellous bony core of the horn. Modified and reproduced with permission [39]. Copyright 2011, Elsevier.	33

## Disclaimer

The contents of this report reflect the views of the authors, who are responsible for the facts and the accuracy of the information presented herein. This document is disseminated in the interest of information exchange. The report is funded, partially or entirely, by a grant from the U.S. Department of Transportation's University Transportation Centers Program. However, the U.S. Government assumes no liability for the contents or use thereof.

## Abstract

Roadside safety hardware, such as longitudinal barriers and crash cushions, is part of the highway infrastructure that is used to protect an errant vehicle from crashing into fixed roadside objects in a well-controlled manner. Despite constantly improved design and standardized full-scale impact testing of the roadside safety hardware, more than 3% of U.S. traffic fatalities are caused by the inefficiency of the roadside safety hardware. Innovative designs are urgently needed to improve the level of safety and decrease the severity of accidents. In nature, many plants and animals are optimized to adapt to various overload conditions and have demonstrated superior impact-resistant and energy-absorbing capabilities. Careful examination of these biological structures may inspire a new generation of roadside safety structural designs. This project comprehensively reviews the structure-property-performance relationship of the exemplary biological materials and demonstrates that the strategies used by the various biological role models can be understood, abstracted, modified, and transferred to bio-inspired roadside safety hardware.

## Chapter 1 Introduction

A vehicle could run off the road due to driver fatigue, excessive speed, crash avoidance, pavement deterioration, vehicle component failure, and poor visibility, among other reasons. An errant vehicle may reach a roadside hazard, collide, or overturn; all of which may result in injuries or even fatalities. In the United States, more than 50 percent of traffic fatalities each year are caused by an errant vehicle crashing into a roadside hazard, such as trees and utility poles [1]. This type of crash, called roadway departure or run-off-the-road collision, constitutes a significant segment of vehicle-related fatalities on higher classification roadways, such as interstates and arterials, which have speed limits from 50 mph to 75 mph [2]. Errant vehicles pose a danger to not only their operators but also to the environment around them. For example, an errant vehicle reaching the opposite side of a dual carriageway can cause serious harm to the people travelling on the other side.

These casualties may be reduced by making every roadside flat, traversable, and obstacle-free, providing enough space to errant vehicles to regain control and return to the road with a reduced likelihood of injury. However, this is not always possible due to either physical or economic constraints. Due to a wide range of roadside objects that cannot be removed, relocated, or made passively safe, the American Association of State Highway and Transportation Officials (AASHTO) adopted multiple approaches to alleviate the damaging consequences of run-off-road collisions, one of which is the utilization of roadside safety hardware [3]. Roadside safety hardware, first came into focus in the 1970's in the United States [2] and is currently part of the highway infrastructure that is widely used across the globe, protecting errant vehicles from crashing into fixed roadside objects through a well-controlled process. It is important to note that roadside safety hardware, although designed to provide controlled impact, is a hazard itself and



should be used as a last resort and only when the consequences of hitting the roadside safety hardware is less than that of impacting the hazard.

In the United States, roadside safety hardware needs to go through a series of standardized full-scale impact tests in accordance with the requirements of NCHRP350 [4] and MASH [5] prior to its use. MASH has superseded NCHRP350 since January 2011. In European countries, EN1317 [6] is adopted instead. These impact tests not only prove whether a hardware performs satisfactorily under certain impact conditions, but they also provide a controlled way of accurately measuring certain impact characteristics of the system under test, such as dynamic deflection, working width, zone of intrusion, and impact severity levels, providing vital information for the hardware designer. Historically, roadside safety hardware systems were primarily developed by the national road authorities and the available systems on the market were limited to a few designs. Over the last few decades, with the development of standardized impact testing systems, the number of trademarked systems developed by private companies has far surpassed that of the non-trademarked ones.

## Chapter 2 State of the Art of Roadside Hardware Design

Roadside safety hardware includes longitudinal barriers, crash cushions, and breakaway supports for signs, luminaires, and traffic signals [7]. In this section, the two most important types will be reviewed, i.e., longitudinal barriers and crash cushions. Like other safety hardware, they primarily serve to lessen the severity of an impact rather than prevent impacts from occurring in the first place.

### 2.1 Longitudinal Barrier

#### *2.1.1 Types and Components of Longitudinal Barrier*

A longitudinal barrier is a device generally placed parallel to traffic flow, as shown in Fig. 1, providing a physical constraint that a vehicle is unlikely to pass. It functions to capture or redirect an errant vehicle away from potential hazards. Two important components of a longitudinal barrier system include a terminal and a transition. A barrier terminal is a crashworthy device used at the end of a longitudinal barrier, preventing errant vehicles from crashing into the untreated end and anchoring the barrier system to the ground to increase its tensile strength during an impact. A barrier transition is a section of barrier used to produce a gradual stiffening when one type of roadside safety hardware is connected to another. Based on their application, longitudinal barriers can be divided into roadside barriers, median barriers, and bridge railings, and they function to shield errant vehicles from natural or man-made roadside obstacles, prevent errant vehicles from crossing the highway median, and prevent errant vehicles from going over the edge of a bridge structure, respectively.

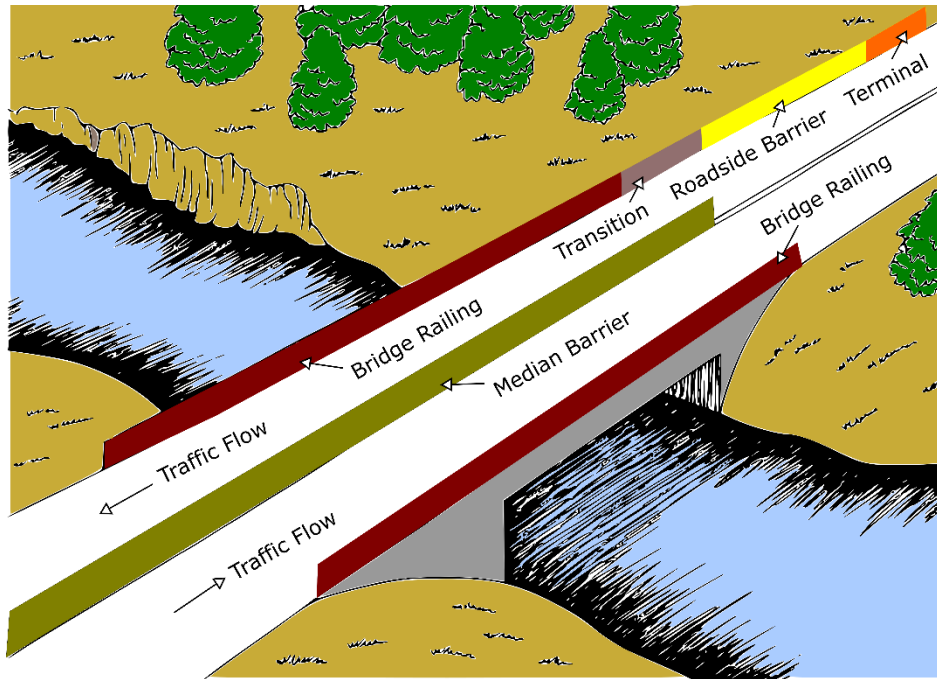


Figure 2.1 Schematic illustration of a terminal, a transition, a roadside barrier, a median barrier, and a bridge railing. This figure is not drawn to scale and for demonstrative purposes only.

A barrier terminal, also known as end treatment, is used at any location where the untreated end of a barrier poses a high risk of injury to vehicle drivers. When the end of a barrier is located within the clear zone and faces oncoming traffic, it is more likely to be hit head-on by an errant vehicle. An errant vehicle impacting the unprotected end may come to a sudden stop, be penetrated by the barrier parts, or roll over. Based on design principles, the terminals can be divided into energy-absorbing terminals and non-energy-absorbing terminals. Energy-absorbing terminals are designed to gradually deform, dissipating impact energy, and bring the impacting vehicle to a stop in such a way that risk of injury to vehicle drivers is minimized. Non-energy-absorbing terminals typically do not deform during an impact event and provide an anchorage for the connected longitudinal barrier. For such systems, the longitudinal forces generated within the system in an impact event need to be anchored into the ground to enable the barrier system to contain and redirect the impacting vehicle.

A barrier transition is used where one type of roadside safety hardware is required to be connected to another to provide a gradual change in stiffness, height, profile, and containment between them. It is generally used between two barrier systems of different rigidity, between a barrier and a terminal, or between a barrier and a fixed rigid object, such as a bridge pier. Without a correctly designed transition, there is a risk of an abrupt change in deflection performance characteristics, potentially leading to vehicular pocketing, snagging, or penetration at the connection. Pocketing means that the system at one end of the transition may deflect so much upon impact that the impacting vehicle then strikes the more rigid system connected at the other end of the transition.

A roadside barrier is a longitudinal barrier used to shield errant vehicles from natural or man-made obstacles located along either side of a roadway by either containing or redirecting the impacting vehicles. They are also used to separate pedestrians and bicyclists from vehicular traffic. Roadside barriers are more often used on highways than any other roadside safety hardware. A roadside barrier is typically placed as far from the roadway as conditions permit while ensuring that the system performs properly. Such arrangement gives an errant vehicle the best chance of regaining control of the vehicle without hitting the barrier.

A median barrier separates opposing traffic on a divided highway and redirects errant vehicles striking either side of the barrier. Median barriers significantly reduce the severity of cross-median crashes, attributed to the relatively high speeds that are typical on divided highways. Approximately 8% of all fatalities on divided highways are due to head-on crashes. One major consideration about median barriers is their width. In the past, median barriers were typically only used when medians were less than 30 feet wide, but many states were

experiencing cross-median fatal crashes in medians wider than 30 feet. Since 2006, AASHTO has been encouraging the consideration of barriers in wider medians [3].

A bridge railing is designed to provide for public safety along the length and edges of a bridge. This includes redirecting errant vehicles back into the roadway without presenting a safety hazard when struck and ensuring the safety of bicyclists and pedestrians. Bridge railings differ from typical roadside barriers because they are more rigid, which is the reason why a transition is often required as the connection between the two provide a smooth change in stiffness. Since the use of transitions was emphasized by the Federal Highway Administration (FHWA), the portion of single-vehicle accidents at the end of bridge railings has been significantly decreased from 52% to 13% and 57% to 25% in California and Texas, respectively [8].

### *2.1.2 Examples of Longitudinal Barrier*

The wire rope safety barrier system, also known as a cable barrier system, normally comprises three or four strands of tensioned cable, held in the designed heights by flexible posts. The design principle is the redirection of the impacting vehicle once sufficient tension is developed in the cables. Most of these systems are designed to contain impacts from both sides and are therefore commonly used as median barriers. One example is MashFlex, a trademarked system from Blue Systems, as shown in Fig. 2(a). It can be seen that, for such systems, the terminals are an integral part of the system, and thus it is not possible to combine these systems with terminals of other makes and models. The terminals are non-energy-absorbing and only act as anchors. The end anchors are held in place by safety cables, preventing the anchors from being thrown into traffic when they become detached.

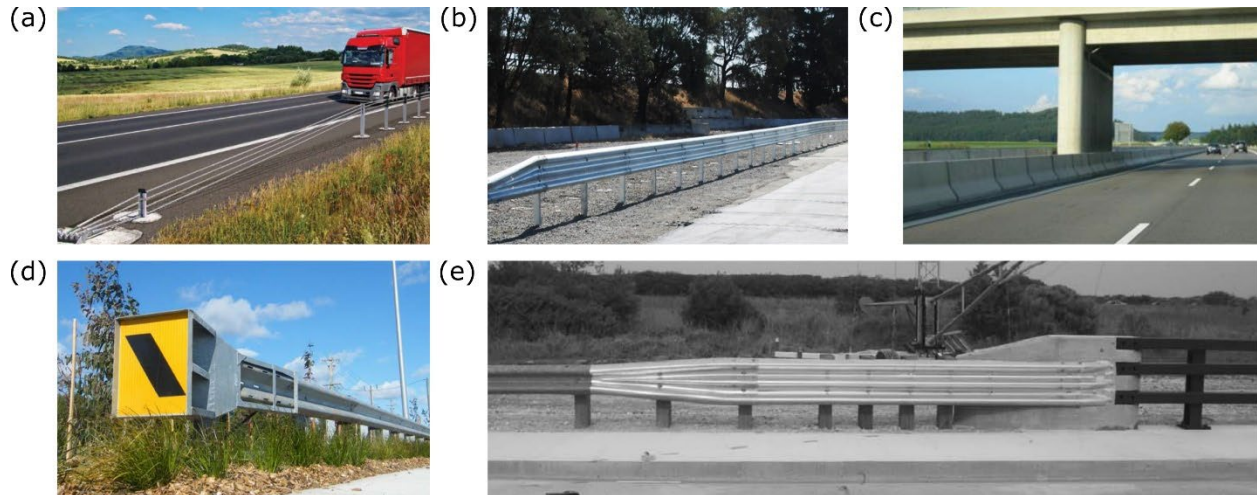


Figure 2.2 Examples of longitudinal barrier include (a) MashFlex [9], (b) Sentry [10] (c) REBLOC [11], (d) SKT-SP [12], and (e) NETC Massachusetts Transition [13].

The w-beam and thrie-beam barrier system also deforms upon impact but to a lesser extent than the wire rope barrier system. When struck by an errant vehicle, the support posts are designed to bend and the barrier rail to deform and act as a belt to absorb some of the impact force. The tensile forces developed in the barrier rail assist in redirecting the impacting vehicle. The thrie-beam is known to provide increased rigidity compared to the w-beam, but the overall performance of these systems changes from one design to another. The double-sided versions of these systems are often used in the medians since they can withstand impacts from both sides. One example from these barriers is Sentry, a trademarked system from Australian Construction Products, as shown in Fig. 2(b). In this particular case, the terminal was formed by sloping the ends of the barriers from full height to the ground level. This type of terminal is non-energy-absorbing and may cause errant vehicles to overturn, launch in the air, or even land on the hazards behind the barrier, and is thus not generally recommended at locations where they are very likely to get hit.

The concrete barrier system does not deflect or deform to a significant extent upon impact, and thus it is often used at locations where there is a very limited width for barrier deflection or where the risk to third parties is greater than that to vehicle drivers. Concrete barriers may have different profiles, such as the F-shape profile, New Jersey profile, and vertical wall profile, leading to different redirection characteristics. Concrete systems are generally known for their ability to contain heavier vehicles, so they are often used as bridge railings. However, these systems are heavy and introduce a permanent load on the bridge, which should be taken into account during the bridge design. One example from these systems is REBLOC, a trademarked system from De Bonte, as shown in Fig. 2(c).

The SKT-SP terminal is a trademarked system from Road Systems. It is designed as an energy-absorbing terminal directly attached to the w-beam barrier to minimize the severity of impacts occurring at the end of the barrier system. The terminal features a slotted anchor rail, an impact head, bolted hinged posts, and a cable assembly, as shown in Fig. 2(d). During head-on impacts, the SKT-SP impact head slides over the w-beam barrier. The w-beam barrier is sequentially kinked or bent as it moves through the head. The kinked barrier exits the head safely and the vehicle is brought to a controlled stop. When impacted along the side, the SKT-SP functions like a longitudinal barrier, and the errant vehicle is safely redirected back toward its original travel path.

The NETC Massachusetts Transition is a barrier transition developed and tested by the New England Transportation Consortium (NETC). It serves as a connection from a w-beam guardrail to a steel bridge railing. The bridge railing consists of three tubular rail elements mounted on wide flange posts bolted to a concrete sidewalk. This transition features four primary elements, including a w-beam to three-beam transition with decreased post-spacing, a two-layer

three-beam section with further decreased post-spacing, a terminal connector, and a shaped concrete buttress, as shown in Fig. 2(e). The shaped concrete buttress serves as a transition from the three-beam section to the bridge railing. The top surface on the leading end of the buttress gradually tapers from 31 inches to 42 inches in height as it approaches the bridge railing. The buttress also features a double taper on the front face at the leading end to mitigate potential vehicular snagging points during impact events.

## 2.2 Crash Cushion

### *2.2.1 Types of Crash Cushion*

Crash cushion, also known as impact attenuator, is a crashworthy safety device designed to protect errant vehicles from the high severity outcomes of impacting fixed objects. Similar to energy-absorbing terminals, this is achieved by gradually decelerating the impacting vehicle to a safe stop before it reaches the fixed hazard. However, unlike terminals that are connected to the end of longitudinal barriers, crash cushions are stand-alone objects. They are always considered at locations where fixed objects within the roadside clear zone cannot be relocated, removed, or longitudinal barrier systems cannot be safely introduced. The use of crash cushions, in comparison to longitudinal barriers, is potentially more appropriate for protecting fixed objects, especially those at exit ramps, gores, ends of median barriers, bridge piers, and bridge abutments.

Originally, crash cushions were empty oil drums systematically placed in front of a fixed roadside object. This basic concept has later evolved to plastic buckets filled with different weights of sand, which are still widely used today. With further development, a wide range of designs are available on the market to date. Based on design principles, the systems currently in use can be divided into the systems designed according to the work-energy principle and the systems designed according to the conservation of momentum principle; based on performance characteristics during frontal impacts, the systems can be divided into gating systems and non-



gating systems; based on performance characteristics during side impacts, the systems can be divided into redirective systems and non-redirective systems; and depending on maintenance characteristics, the systems can be divided into sacrificial systems, reusable systems, and self-restoring systems.

The systems designed according to the work-energy principle utilize crushable or deformable components to convert the kinetic energy of the impacting vehicle into other forms of energy. Some of the kinetic energy of the vehicle is transformed to mechanical energy via the deformation of the vehicle and crash cushion components, and some of these components convert the mechanical energy into potential energy and deform back to their initial shape at the end of the impact, similar to a spring. Some of the kinetic energy of the vehicle is transformed to thermal energy by the friction between the system components and the vehicle. And some of the kinetic energy is transformed to acoustic energy through the noise generated during the impact. Most of the crash cushions available on the market today are designed according to the work-energy principle.

The systems designed according to the conservation of momentum principle utilize materials of expendable mass, such as sand and water, to which the kinetic energy of the impacting vehicle can be transferred during the collision. The material of expendable mass is often kept in containers such as drums or buckets. As the impacting vehicle collides with each container, the expandable mass located inside the container is shifted and dispersed around the crash by the transfer of momentum from the vehicle to the mass. A typical arrangement involves an increasing amount of mass within each row of containers and the number of containers also increases towards the back. The net effect of this layout is a gradual increase in the amount of mass within the system to ensure a gradual decrease of speed for the impacting vehicle. In

comparison with the systems designed according to the work-energy principle, they occupy considerably more space and need more repair work, but they can be moved more easily from one location to another, and thus are often placed in areas that require temporary protection, such as construction sites.

Based on performance characteristics during frontal impacts, the crash cushion systems can be divided into gating systems and non-gating systems. When a vehicle impacts near the nose of the gating system, the system folds away to allow the vehicle to pass safely, similar to a gate, as shown in Fig. 2(a). In contrast, non-gating systems disallow impacting vehicles from passing through the system. Instead, they either arrest or redirect them along the roadway, as shown in Fig. 2(b). As a result, a full clear zone is required behind the gating crash cushions to let the impacting vehicle regain control after gating through the device, whereas a much smaller clear zone is needed behind the non-gating devices. Thus, non-gating devices are typically used in wide medians or roadway shoulders where a sufficient clear zone is not available.

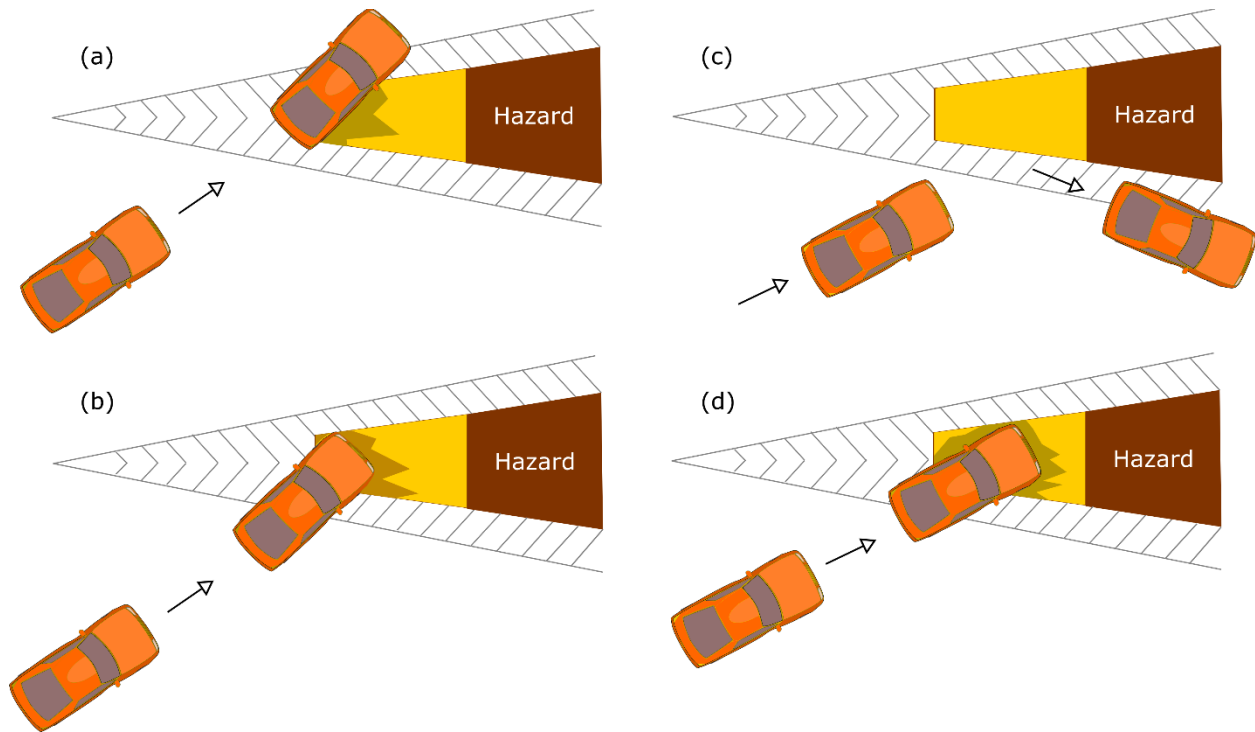


Figure 2.3 Schematic illustration of (a) a gating system, (b) a non-gating system, (c) a redirective system, and (d) a non-redirective system. A hazard is a roadside feature or object that can cause physical or economic harm or loss if reached by an errant vehicle.

Based on performance characteristics during side impacts, the crash cushion systems can be divided into redirective systems and non-redirective systems. When impacted by a vehicle on the side, redirective systems redirect the vehicle along the roadway to the direction it was originally traveling, as shown in Fig. 2(c), whereas non-redirective either allow the vehicle to pass through or contain the vehicle within the system, as shown in Fig. 2(d). While redirective systems can be either gating or non-gating, non-redirective systems are predominantly designed according to the conservation of momentum principle, i.e., the barrel and sand systems, and therefore they are predominantly gating systems.

Crash cushions can also be categorized into three systems, i.e., sacrificial systems, reusable systems, and self-restoring systems, depending on the amount of repair work required to return the system to a crashworthy state after an impact event. Sacrificial systems are designed

for a single impact before requiring significant repair and replacement of components. Due to the low initial cost but greater level of repair required, sacrificial crash cushions should only be used in areas where the risk of impact is low. For reusable systems, some of the major components have been designed to be reusable after an impact, but some of the components need to be replaced after an impact to ensure that the crash cushion is maintained to produce the original level of performance in a subsequent impact. Self-restoring systems experience very little, if any, damage during impact events and are designed to be easily recovered to their original condition. They are generally made of more durable materials, such as high-density polyethylene, and thus can typically stand up to multiple impacts and dramatically reduce the need for repeated repair or replacement. There are relatively high levels of cost associated with the initial purchase and installation of such self-restoring systems, but there are subsequent low levels of repair and maintenance. At highway locations which suffer frequent impacts, self-restoring cushions are always preferred to reduce the risk to road users, as numerous fatality cases were caused by vehicle collision with already-crushed crash cushions [14].

### *2.2.2 Examples of Crash Cushion*

The ENERGITE III crash cushion is a trademarked system from Energy Absorption Systems. It is a gating, non-redirective, and sacrificial system designed according to the conservation of momentum principle. It consists of a series of modules filled with different weights of sand, as shown in Fig. 2(a). Each module includes a barrel, a lid, and a cone insert to modify the center of mass and total weight of the module.

The RAPTOR crash cushion is a trademarked system from Barrier Systems. It is a gating, non-redirective, and sacrificial system designed according to the work-energy principle. It uses weather-resistant energy-absorbing material surrounded by a polyethylene shell to shield poles

and trees located on the roadside, as shown in Fig. 2(b). It can be installed at many sites that do not have sufficient space needed for a traditional crash cushion.

The EASI-CELL crash cushion is another trademarked system from Energy Absorption Systems. It is a gating, non-redirective, and self-restoring system designed according to the work-energy principle. It consists of a configuration of high-density polyethylene cylinders, as shown in Fig. 2(c). The cylinders compress to maximize energy absorption during an impact and recover a significant portion of their original shape and capacity without maintenance or repair after the impact.

The HEART crash cushion is a trademarked system from Trinity Highway Products. It is a non-gating, redirective, and self-restoring system designed according to the work-energy principle. The system features a configuration of steel diaphragms arranged on tubular steel tracks and enclosed by a series of high-density polyethylene side panels, as shown in Fig. 2(d). During frontal impacts, tension cables attached to the second diaphragm are released and the assembly moves towards the back, crushing the high-density polyethylene side panels to absorb the kinetic energy of the impacting vehicle. For side impacts, the tubular steel tracks provide the necessary lateral restraint to direct vehicles.

The Universal TAU II crash cushion is another trademarked system from Barrier Systems. This is a non-gating, redirective, and reusable system designed according to the work-energy principle. It consists of steel diaphragms dividing the assembly into collapsible bays, sliding panels, and energy-absorbing cartridges, as shown in Fig. 2(e). The assembly collapses rearwards during frontal impacts, crushing the energy-absorbing cartridges in the first bay and dispensing the impact forces uniformly to the other cartridges via the diaphragms until the vehicle reaches a significantly lower speed. During side impacts, the steel cables running along

the length of the system underneath the diaphragms resist the lateral movement and assist directing the vehicle. Energy absorbing cartridges in each bay must be replaced after each crash to maintain effectiveness.

The ADIEM crash cushion is another trademarked system from Trinity Highway Products. It is a gating, redirective, and sacrificial system designed according to the work-energy principle. It is a narrow crash cushion comprised of two major components, i.e., a wedge-shaped base and ten lightweight, crushable concrete modules, as shown in Fig. 2(f). A side pipe rail is cast on the base to help direct the impacting vehicle back to the direction it was originally traveling. Because the lightweight concrete is porous, the modules are coated by acrylic latex to protect them from moisture.

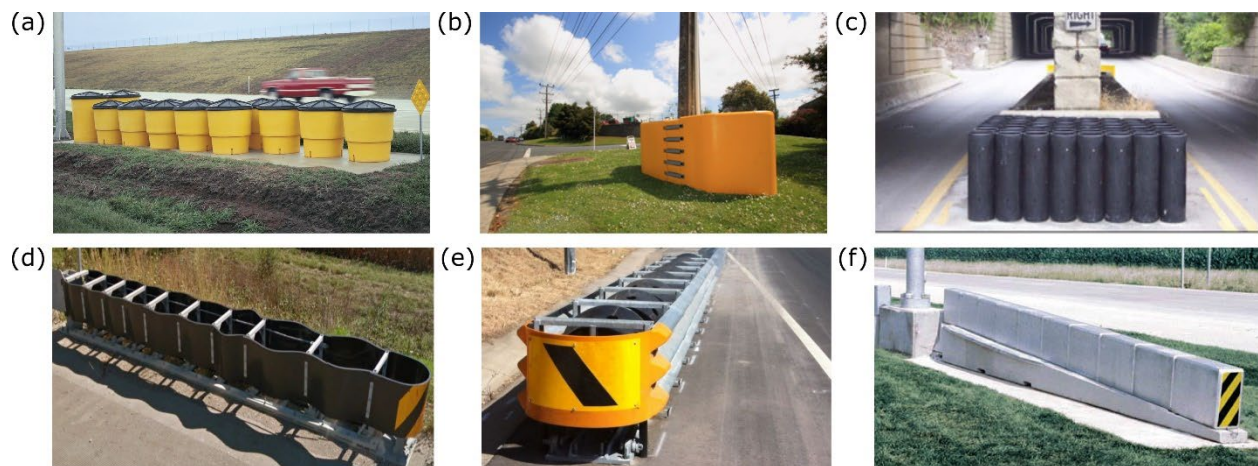


Figure 2.4 Examples of crash cushion include (a) ENERGITE III [15], (b) RAPTOR [16], (c) EASI-CELL [17], (d) HEART (The picture is from Google Street View), (e) Universal TAU II [18], and (f) ADIEM [19].

### 2.3 Current Issues and Challenges

Despite improved design and standardized crash testing of roadside safety hardware, more than 3% of U.S. traffic fatalities are caused by the inefficiency of the roadside safety

hardware, according to the National Highway Traffic Safety Administration (NHTSA)'s Fatality Analysis Reporting System Database [7]. Although private manufacturers constantly improve their designs to position themselves ahead of their competition within the market, most of the improvements are incremental and the past decade saw no significant changes. In addition, a vast majority of the roadside safety hardware are not designed with motorcycles in mind, i.e., they do not specifically function to stop errant motorcycle riders from reaching the roadside hazards and even become a risk to the riders due to exposed posts, sharp edges, and corners [20].

Furthermore, due to the increased environmental awareness of the general public and the decreased price of lithium-ion batteries, there has been a rapid growth of the market of electric vehicles in the last decade. Electric vehicles come in various shapes and sizes, whose weight, height, and the position of the center of mass are different from those of conventional vehicles, but the roadside safety hardware and the standardized impact testing are not designed to consider electric vehicles. How to improve current systems to accommodate electric vehicles remains a complete blind spot.

### *2.3.1 Issues for Motorcycles*

The current design of roadside safety hardware does not account for motorcycle riders, and the design of longitudinal barriers has a particularly significant contribution to the motorcycle fatalities. It has been estimated that motorcycles account for 42% of all fatalities resulting from collisions with steel guardrails, and 22% resulting from collisions with concrete barriers [20]. Approximately 12% of the motorcycle riders who crashed into a steel guardrail died in the event; the fatality rate is 80 times higher than that for automobile drivers [20]. There are two dominant types of accidents between motorcycles and longitudinal barriers. In the first type, motorcycle riders hit the barrier while sliding on the ground, having dismounted from their motorcycle. The impact mainly occurs with the lower section of the barrier. In the second type,

riders hit the barrier at an upright position while they are still on the motorcycle, and the impact occurs with the upper section of the barrier.

Steel w-beam or three-beam guardrails are not designed to protect motorcycle riders. Errant riders may slide on the ground and easily go between the posts underneath the rail to reach the hazard behind the barrier. Hitting the barrier itself is not any better, as the exposed barrier posts constitute the leading cause of the accidents between motorcycles and safety barriers [21]. For riders who hit the barrier at an upright position, the sharp corners located at the top of the posts also pose a significant risk. According to the Norwegian Public Roads Administration (NPRA), the posts are particularly hazardous when riders fall from the motorcycle during an impact and hit the top of the posts [22]. Wire rope barriers pose a similar level of danger due mainly to the exposed posts rather than the wire ropes. There was no significant difference in the percentage of killed or seriously injured riders of those involved in motorcycle collisions with steel guardrails and wire rope barriers [23]. Concrete barriers do not feature any sharp edges or corners, making it a safer choice for motorcycle riders. In addition, it does not let errant riders pass through and strike hazards located behind the barrier. On the other hand, the risk of head injury is the leading mode of injury resulting from motorcycle accidents with concrete barriers[24].

Although there are currently several trademarked motorcyclist protection systems available on the market, there exists no standardized crash test methodology for such systems, according to either NCHRP350 or MASH. Only the European EN1317 provides standardized impact testing to assess their performance, but it addresses only the sliding mechanism, which is far from being comprehensive, as approximately 50% of motorcycle riders were in an upright position when they hit the barrier [25]. It can be concluded that innovative ideas are urgently



needed to design motorcyclist protection systems, improve existing roadside safety hardware to provide sufficient protection for motorcycle riders, and update the crash testing guidelines to include a standardized assessment for such systems.

### *2.3.2 Issues for Electric Vehicles*

The design of crash cushions has experienced incremental changes in the past decade, but automobiles have evolved significantly over the years. The most notable is the advent of electric vehicles and the recent acceleration of electric vehicle adoption. In 2020, more than 10 million electric vehicles were on the roads across the globe [26]. Electric car registrations increased by 41% in 2020 when the global vehicle sales dropped approximately 16% due to the COVID-19 pandemic [26]. Electric bus and electric truck registrations also grew significantly, reaching global stocks of 600 thousand and 31 thousand, respectively [26]. As the number of countries announcing commitments to accomplishing net-zero emissions over the next decade keeps increasing, the International Energy Agency (IEA) predicts that half of all vehicles sold globally will be electric by 2035 [27]. With such a tremendous increase, the question that must be posed is what new safety issues electric vehicles will bring about in comparison with conventional gasoline-powered vehicles.

While the outstanding performance of electric vehicles and superior reliability of the driver assistance systems do have the potential to make our world a much safer place, the cases of run-off-road collisions actually increased during the past few years and will continue to increase for the foreseeable future. AXA, a French insurance company, recently has shown that, although the claim frequency of electric vehicles is generally comparable to that of conventional vehicles, the claim frequency of electric sport utility vehicles and luxury vehicles is approximately 40% higher than that of their conventional counterparts [28]. Topdanmark, a Danish insurance company, has shown that electric vehicles are involved in 20% more accidents

than their conventional counterparts; for Tesla, the number is as high as 50% [29]. In Norway, approximately 50% of electric vehicle owners have an accident within the first year compared 25% for conventional vehicles [29].

This could be due to the fact that some features of electric vehicles place higher demands on road users, such as rapid acceleration, silent engine, and utilization of driver assistance systems. Electric vehicles are effective in rapid acceleration typically only seen in high-end gasoline-powered vehicles, and thus many fatalities were caused by sudden “unintended acceleration” when drivers confused the brake pedal with the accelerator pedal [30]. Another feature of electric vehicles is that their propulsion noise is much quieter than their internal combustion engine counterparts, and thus drivers and pedestrians are not alerted to approaching vehicles [31]. Moreover, due to reliance on the driver assistance systems, a driver does not need to always concentrate on the traffic; when the assistance system reaches the limit of its capacities and immediately gives the driving task back to the driver, the driver may react too late. Numerous cases of accidents are known to have been caused by the driver’s overreliance on the driver assistance systems [28]. It can be seen that, during our transition to electric vehicles, there will be more run-off-road collisions on roads in the upcoming years, and thus higher demands will be placed on the utilization of roadside safety hardware.

However, current state-of-the-art roadside safety hardware and standardized impact testing are not designed to consider electric vehicles, and how to improve current systems to accommodate the unique features of electric vehicles remains a blind spot. Electric vehicles come in various shapes and sizes, whose weight, height, and the position of the center of mass are different from those of conventional vehicles. For example, electric vehicles generally weigh considerably more than their gasoline-powered counterparts due to the presence of heavy

lithium-ion battery packs [32]. The GMC Hummer Edition 1 weighs over nine thousand pounds, roughly three times the weight of a Honda Civic [32]. The Ford F-150 Lightning weighs about 1.6 thousand pounds more than a similar gasoline-powered F-150 truck [32]. The electric Volvo XC40 Recharge weighs about one thousand pounds more than a gasoline-powered Volvo XC40 [32]. Heavier vehicles put higher demands on the design of roadside safety devices, since more kinetic energy will be transferred to them during a collision. Although electric vehicles may become lighter over time due to the ever-increasing energy density of lithium-ion batteries, the design of roadside safety hardware should be improved to enhance its performance for the near future.

While lithium-ion batteries with increased energy density could reduce the weight of an electric vehicle, the drawback is that accidents involving electric vehicles will be more deadly due to uncontrollable explosion of the battery packs. It is generally recognized that vehicle crashes involving the intrusion of foreign objects into the battery pack will quite possibly lead to thermal runaway, fire, and explosions. While battery packs in hybrid vehicles are relatively small and typically arranged in well-protected zones, plug-in hybrids and purely electric vehicles use much bigger battery packs. In some designs, such as Fisker Karma, Chevy Volt, and Opel Ampera, battery packs are arranged along the tunnel between the seats and in the region of the rear axle under the passenger seat, where fuel tanks are located in most gasoline-powered vehicles; and in many other designs, such as the BMW i3, Nissan Leaf, Mitsubishi i-MiEV, and Tesla Model S, battery packs are placed under the vehicle floor, which provides ample interior space for passengers but lowers vehicle ground clearances. The widely publicized accidents of the Tesla Model S that caught fire after hitting road debris demonstrates the grave consequence of this design [33]. Thus, the roadside safety hardware systems should be improved to account

for the safety of the battery packs and the crash testing guidelines should be updated to incorporate the standardized assessment for such systems.

The above-mentioned issues have important implications for the design of roadside safety hardware. It can be concluded that innovative designs with superior energy-absorbing and impact-resistant capabilities are urgently needed to decrease the severity of accidents for various types of road users. New designs may be more expensive to manufacture and more time-consuming to install than conventional ones, but the additional level of safety provided for all road users may justify their application. Well targeted roadside safety improvements are always considered to be highly beneficial investments.

## Chapter 3 Biology as Inspiration for the Design of Crash Cushions

In nature, many plants and animals are optimized to adapt to various overload conditions and have demonstrated superior impact-resistant and energy-absorbing capabilities. Careful examination of these biological structures may inspire a new generation of roadside safety structural designs. This section will comprehensively review the structure-property-performance relationship of the exemplary biological materials and demonstrate that strategies used by biological role models can be understood, abstracted, modified, and transferred to bio-inspired crash cushions.

### 3.1 Exemplary Biological Materials

In this section, four biological role models, including tree bark, coconut endocarp, sea urchin spines, and bovid horn, are chosen from nature for their differing strategies in dealing with mechanical impacts. The tree bark demonstrates an impressive damping capability due to its fibrous nature and multi-layered hierarchical structure; the coconut endocarp uses crack deflection, crack branching, and crack trapping as strengthening and toughening mechanisms of impact protection; the sea urchin spines possess a very high initial crushing strength and significant energy dissipation via graceful-failure fracture behavior, mainly thanks to its porosity variation; the bovid horn exhibits superior energy-absorbing and load-bearing capacities, mainly attributed to its curved conical shape, core-shell structure, and variations in the mechanical properties along its length direction.

#### *3.1.1 Tree Bark*

Tree bark is the peripheral layer of stems of woody plants, composed of all the tissues located superjacent to the vascular cambium. Due to its outermost position, it fulfills multiple protective functions, e.g., it protects the sensitive cambium from mechanical influences, such as rockfall events, by dissipating a significant portion of impact energy [34]. The cambium is a thin

formative layer that produces new cells, in charge of the secondary growth of both xylem and phloem, and it cannot be reformed after damage. Thus, protecting the vascular cambium is vital for the survival and development of the entire organism. During rockfall incidents, both the tree bark and the cambium could be injured thanks to the significant mechanical influences, especially for the tree species with thin barks. Even when the injury is not fatal, subsequent infestation caused by bacteria or fungi that enter the tree via the injury can be a serious threat for the entire plant. In a recent study [35], the protective capability of the bark of the tree species native to regions with constant rockfall activities, e.g., *Sequoiadendron giganteum*, as shown in Fig. 3(a), has been compared to that of the bark of the tree species that are native to flat areas with almost no rockfall incidents, e.g., *Ailanthus altissima*, which provides important insight on how the structure and composition of a tree bark determines its energy dissipation capability.

The tree bark of *S. giganteum* consists of a thin inner bark enclosed by a thick outer bark, as shown in Fig. 3(b). Long fibers arranged in layers can be observed from the outer bark. Based on the X-ray computed tomography ( $\mu$ CT) images of the cross-section of the outer bark, the layers are observed on two hierarchical levels. On the lower hierarchical level, the distance between adjacent layers typically equals several hundred microns, as denoted by the arrowheads in Fig. 3(c), and they are nearly parallel to each other. On the higher level, the layers are approximately a few millimeters away from each other, as denoted by the arrows in Fig. 3(c). Microscopic views of the colored thin sections show that the inner bark is interspersed with layers of thick-walled fiber cells and thin-walled parenchymatous cells, as shown in Fig. 3(d). The fiber cells have considerably lignified cell walls, occupying almost the entire cell, as shown in Fig. 3(e). These fibers possess a rectangular cross-section, and neighboring cells are connected via the short side of the rectangle. Each layer of the fiber cells contains a single cell, whereas

multiple layers of parenchymatous cells are often distributed between them. The outer bark also has this configuration, as shown in Fig. 3(f), where thick-walled cells are connected to the neighbors via the short side of the rectangular cross-section. However, unlike the inner bark, the parenchymatous cells are completely dried due to their fractured cell walls; and the fiber cells are considerably elongated, as shown in Fig. 3(g).

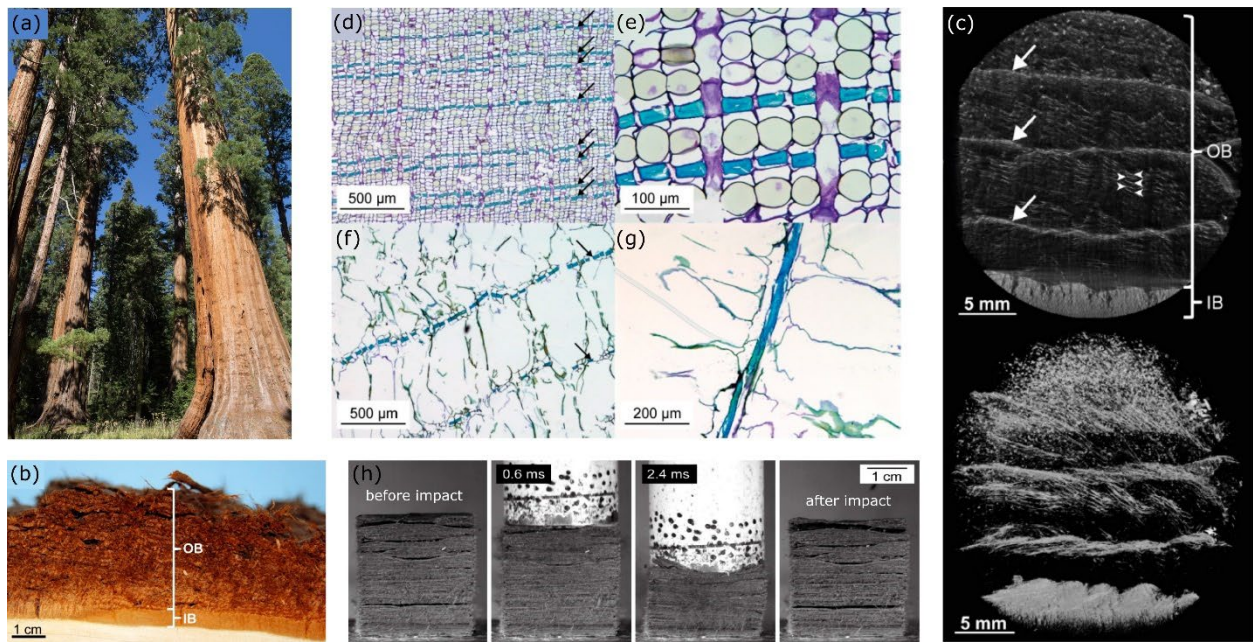


Figure 3.1 (a) *S. giganteum* in Sequoia National Park, California, USA. (b) The tree bark of *S. giganteum*, consisting of a thin inner bark (IB) enclosed by a thick outer bark (OB). (c)  $\mu$ CT of the cross-section of the outer bark. (d) A cross-section of the inner bark. (e) An enlarged view of the cross-section of the inner bark. (f) A cross-section of the outer bark. (g) A radial section of the outer bark. (h) Images from a typical drop-weight test of the *S. giganteum* bark. Modified and reproduced with permission [35]. Copyright 2020, MDPI.

The results of dynamic drop-weight tests show that 90.8% of the energy introduced by the impactor is dissipated by the *S. giganteum* bark, whereas only 85.2% of the energy is dissipated by the *A. altissima* bark. This proves that *S. giganteum* bark is considerably more effective in preserving the subjacent sensitive tissues during impact events. Images from a

typical drop-weight test of the *S. giganteum* bark are shown in Fig. 3(h). Initially, merely the spaces between the fiber layers are compressed, and then the layers themselves are compressed, followed by both the fiber network and the fibers themselves. After the impact event, the bark recovers to its initial shape.

It can be concluded that the fibrous nature and the multi-layered hierarchical composition of the tree bark is quite possibly the scientific reason why this botanical damping system dissipates significant amounts of energy. The *S. giganteum* bark is thus a very promising biological role model for the design of crash cushions and energy-absorbing terminals.

### 3.1.2 Coconut Endocarp

The coconut palm, i.e., *Cocos nucifera*, is the most popular variant of palm tree that grows in coastal tropical regions and can extend to approximately 30 m in height. It produces coconuts, which have been used as a food source for more than four thousand years. When coconuts weigh approximately 3.7 kg and drop onto the ground, they experience intense impacts of more than 1 kJ. To guarantee the germination of the embryo inside, they need to endure the impact energy and stay intact to ensure the protection of the embryo from all kinds of microbial infection. All the attributes are guaranteed by the triple-layer pericarp which contains a membranous exocarp, a fibrous mesocarp, and a woody endocarp, as shown in Fig. 4(a). In a recent study [36], the hierarchical composition of the coconut endocarp has been investigated, which occurs on a total of eight hierarchical levels, denoted as H0 to H7, including length scales from 0.1 m for the entire endocarp to the sub-cellular level in the range of 10 nm to 100 nm. These findings provide us a much deeper understanding of the impressive strengthening and toughening mechanisms of the coconut endocarp.

On the H2 hierarchical level, the endocarp, which constitutes the inmost layer of the fruit wall, is ovoid in shape. At the distal end of the endocarp, three distinctive germination pores, i.e.,



micropyles, are situated between three ridges running along the longitudinal axis. The thickness of the endocarp is varied throughout the entire body. The thickest region is located close to the three micropyles, whereas the thinnest area is located on the opposite side of the endocarp. On the H3 hierarchical level, i.e., the tissue level, the endocarp comprises a condensed sclereid cell matrix with a three-dimensional network of less condensed channels, i.e., the vascular bundles, as shown in Fig. 4(b). On the H4 hierarchical level, i.e., the cell level, only the xylem cells can be observed in the vascular bundles of a mature endocarp, and the phloem cells remain merely as broken fragments. The xylem cells are regarded as tracheids, due to their small diameters, i.e., approximately 10 microns, and the absence of perforation plates, which can generally be observed in vessels, as shown in Fig. 4(c). The sclereid cell matrix consists of circular stone cells and prolonged sclereid fibers located parallel to the vascular bundles. The shape of the sclereid cells varies widely, but it has been observed that their length increases and their width decreases along the inward direction. On the H5 hierarchical level, i.e., the sub-cellular level, the tracheids have a polygonal cross-section, and the thickness of the cell wall is a few microns. The sclereid cells have a circular cross-section and their cell walls occupy more than 90% of the cross-sectional area of the cell. On the H6 hierarchical level, the primary cell wall of the sclereid cells has a thickness of a few microns, significantly thicker than the secondary cell wall with a thickness of a few hundred nanometers. The secondary cell wall consists of multiple individual layers connected via pits, as shown in Fig. 4(d).

To better understand the structure-property-performance relationship of the coconut endocarp, Schmier et al. investigated its failure behavior by conducting quasi-static compression tests and dynamic impact tests on different length scales using diverse loading rates [37]. It has been found that the multiscale hierarchical composition provides multiple fracture resistance

mechanisms, as shown in Fig. 4(e) to Fig. 4(g). On the H3 hierarchical level, the vascular bundles bring about crack deflection, crack branching, and crack trapping as toughening mechanisms. In addition, micro-cracks are observed in front of the macro-crack tip in the sclereid cell matrix. On the H4 hierarchical level, the crack is constantly deflected as it goes through the sclereid cells. In addition, wedging created by emerging sclereids generates extra frictional resistance, decreasing the forces at the crack tip. On the H5 hierarchical level, the pits greatly assist hindering the crack from running through the cells by deflecting it into the cell walls. The crack tip is blunted multiple times as each individual cell wall layer fractures. Wedging created by emerging pits also results in toughening the endocarp.

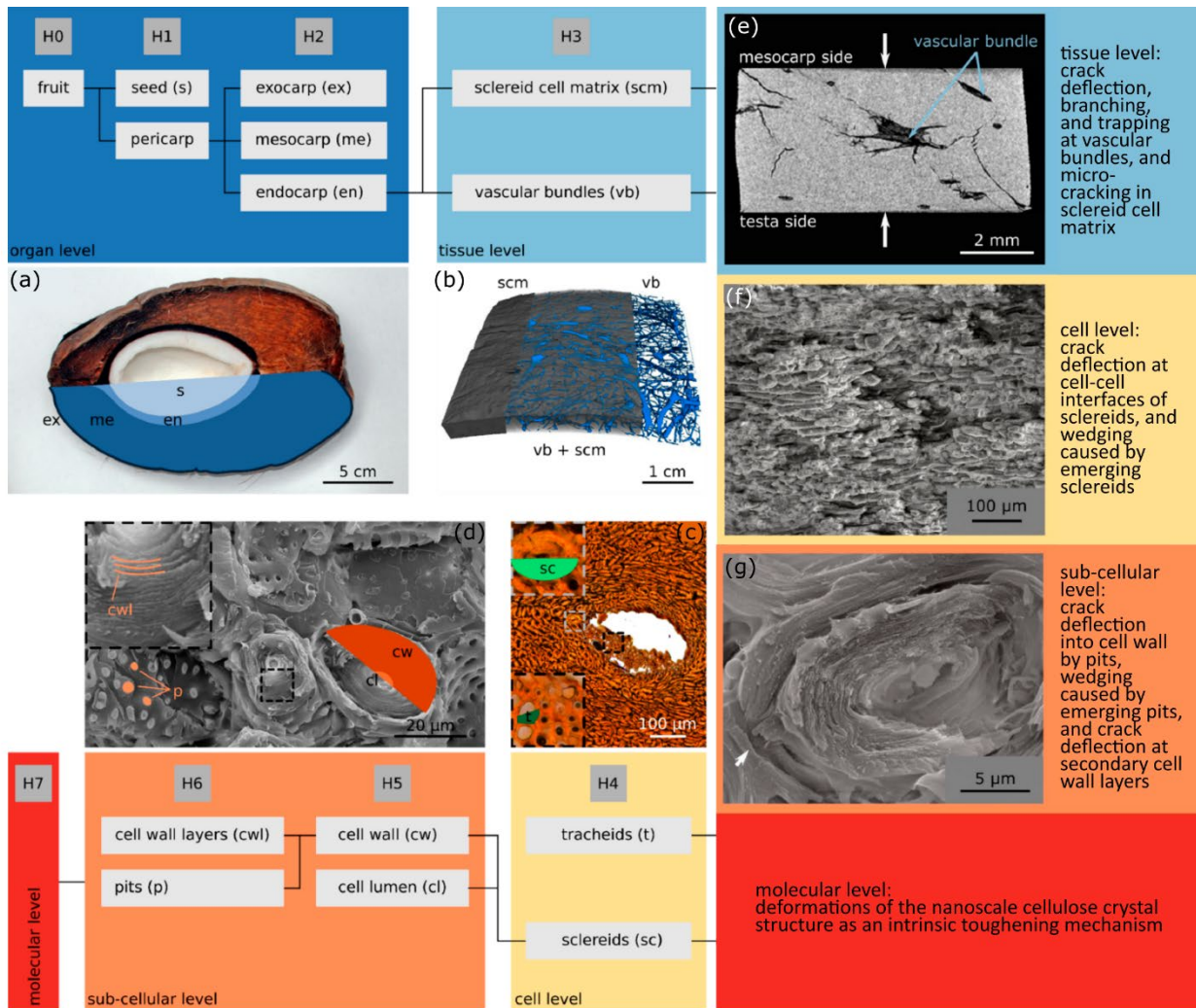


Figure 3.2 The hierarchical composition of the coconut endocarp occurs on a total of eight hierarchical levels, denoted as H0 to H7. (a) A coconut fruit cut in half. (b) A coconut endocarp sample. (c) The cross-section of a vascular bundle in the sclereid cell matrix. (d) The sclereid cell matrix. (e) The cross-section of a fractured endocarp sample tested in compression. (f) A deflected crack in the sclereid cell matrix. (g) A deflected crack in a single sclereid cell. Modified and reproduced with permission [36]. Copyright 2020, MDPI.

Coconut endocarp uses crack deflection, crack branching, and crack trapping as strengthening and toughening mechanisms of impact protection. This hierarchical toughening structure is extremely inspiring and thus serves as a biological role model for the design of impact-resistant longitudinal barriers.

### *3.1.3 Sea Urchin Spines*

About 950 species of sea urchins live on the seabed, inhabiting all oceans and depth zones, from the tide line to more than 16,000 feet deep. Their spherical hard shells, i.e., tests, have long spines that can be up to several inches in length. In the case of an attack by predators, such as sea otters, starfish, wolffish, and triggerfish, the spines protect the spherical test, typically by sacrificing themselves to absorb energy as they break. If the predator impacts axially, the spine pierces the object and snaps off, requiring high strength in compression, and brittle fracture in tension or torsion. If the predator impacts the spine along its length, it absorbs the energy by brittle fracture in bending. In both scenarios, significant portion of the impact energy is absorbed, and the forces are distributed away from the test.

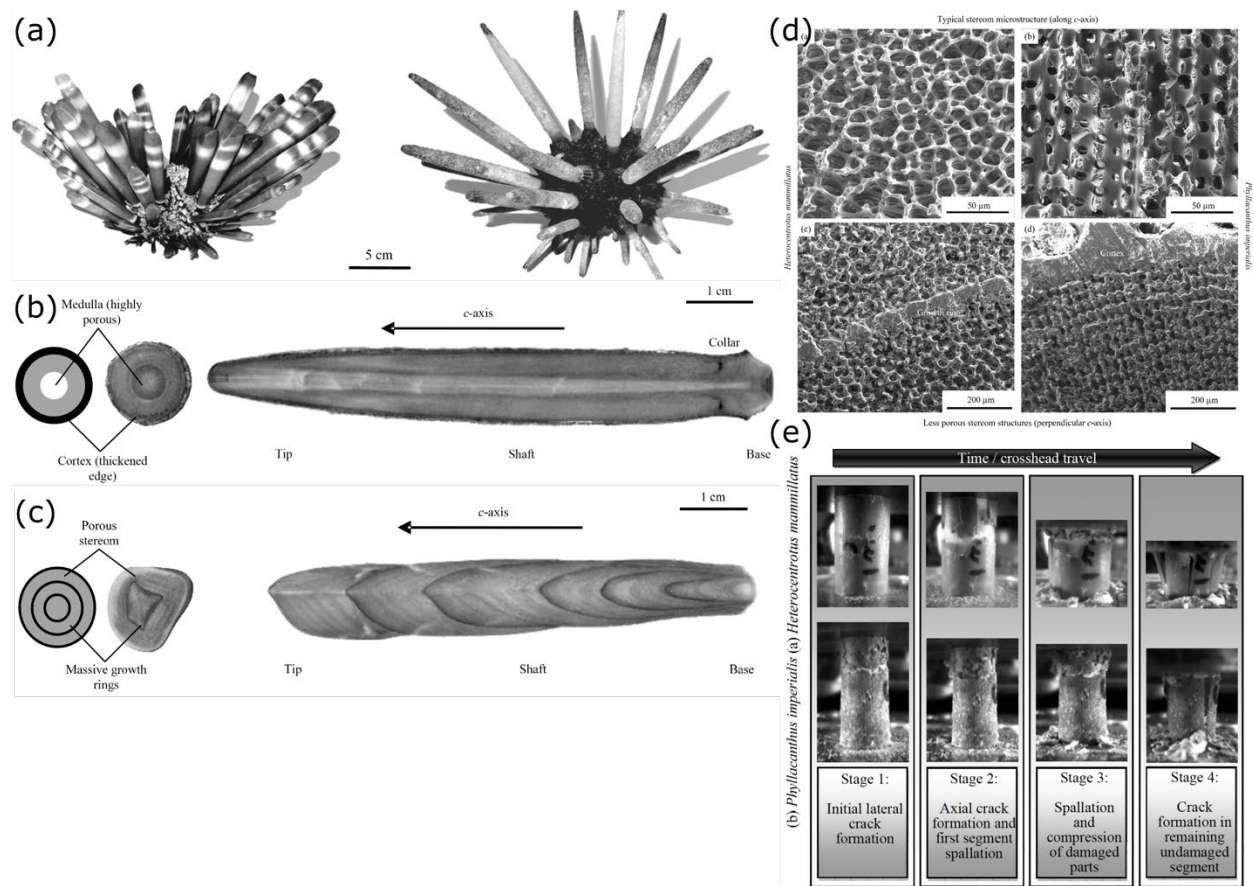


Figure 3.3 (a) Photographs of the studied sea urchin species: *Heterocentrotus mammillatus* on the left and *Phyllacanthus imperialis* on the right. (b) Microphotographs of *Heterocentrotus mammillatus* spine cross sections. (c) Microphotographs of *Phyllacanthus imperialis* spine cross sections. (d) SE-mode SEM images of *Heterocentrotus mammillatus* and *Phyllacanthus imperialis* stereom structures. (e) Microphotographs showing characteristic stages of the fracture behavior of sea urchin spines under bulk compression. Modified and reproduced with permission [38]. Copyright 2009, Elsevier.

The calcite stereom of sea urchin spines is, apart from a dense part on the base, highly porous and shows a complex and diverse structure [38]. The macrostructure of the spines of the studied sea urchins differs significantly, as shown in Fig. 5. Spines of *Heterocentrotus mammillatus* show an internal structure with stereom layers separated by more compact layers, which may be interpreted as former shell surfaces or growth marks. These compact layers, however, are not completely dense but just porous enough to ensure permeability. The individual

sequences of porous and compact stereom structures are often not uniform and the axial center of the spines has an increased porosity, both in the stereom and the separating layers. The top layer of the spine is a thin epidermal bare skin. Spines of *Phyllacanthus imperialis* have a simpler setup comprising a highly porous inner area, a somewhat less porous stereom further out and a highly dense outer edge. The cortex is typically overgrown with small mollusks and calcifying bacteria. The open pore volume varies from almost fully dense to approximately 10 vol% and reaches up to 60 vol% in the rest of the stereom. Typical pore size diameters range between 10  $\mu\text{m}$  and 30  $\mu\text{m}$ .

Under bulk compression, sea urchin spines showed distinct fracture behavior, characterized by graceful failure. In the first phase, spines of both studied sea urchin species show initial formation of horizontal cracks which are limited to the very surface of the samples and which usually run around the whole spine. These initial cracks act either as points of origin for cracks running axially upwards or as a stopper for cracks running from the top down which appears at higher loads. This separates the top part of the specimen into lath-like segments, which eventually spall in the course of further crosshead movement. It can be seen that the sea urchin spines possess a very high initial crushing strength and significant energy dissipation via graceful-failure fracture behavior, mainly thanks to its porosity variation, and thus serves as a biological role model for the design of impact- crash cushions and energy-absorbing terminals.

#### *3.1.4 Bovid Horn*

Most bovid animals, such as cattle, oxen, and antelopes, have a pair of curved and pointed horns on their heads. The horns are used as weapons to compete for territory, hunt for food, and gain the opportunity to mate with females. Cattle with broken horns are socially disadvantaged in the herd due to their vulnerability. During head-on collisions, sheep horns can withstand a maximum impact force of 3400 N [39]. Therefore, as a result of natural selection, the

horns of bovids must have evolved to possess remarkable load bearing and energy absorption capacities.

As shown in Fig. 6, each horn has a curved conical shape. Such a geometric feature is not only necessary for the horn to serve as a powerful sharp weapon to offense and defense, but also leads to a relatively uniform distribution of the maximal stress along its longitudinal direction. From the viewpoint of strength, therefore, the horns approximately follow the optimal structural design rule of “equal strength”, ensuring their biological function of protection. The horns have a core-shell structure, consisting of a keratinous sheath and a bony core. The outer keratinous sheath of the horn has a high fracture toughness, ensuring structural integrity and preventing the rupture of the horn, while the living cancellous bony core, which is relatively brittle, can absorb energy and repair the possible damage occurred during fighting. Such a composite structure can efficiently protect the horn itself in different fighting behaviors. The stronger keratinous sheath plays an essential shielding role and protects the inner bone from damage and fracture. The composition, microstructure and mechanical properties of the horn vary along its length direction, further enhancing the load-bearing ability and structural integrity.

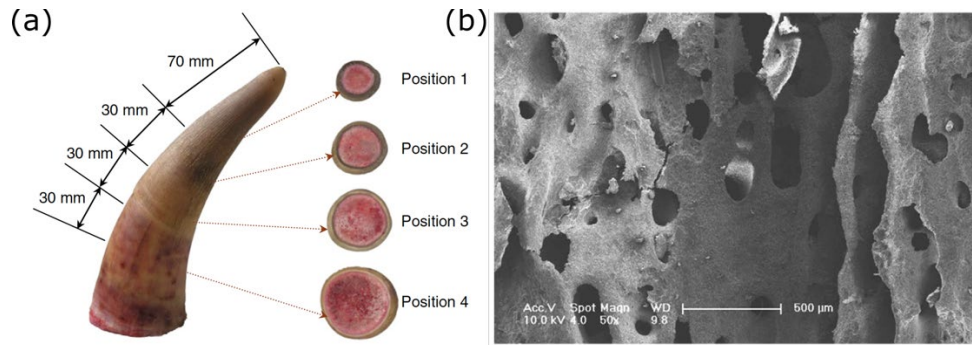


Figure 3.4 (a) Schematic view of the bovine horn and sampling positions. (b) SEM photograph of the cancellous bony core of the horn. Modified and reproduced with permission [39]. Copyright 2011, Elsevier.

The static compression result showed that a single horn can withstand a compressive force up to 7.6 kN, which is high enough for fierce fighting. The mechanical properties of horn piece samples under low and high strain rates were also tested. It is found that the Young's modulus and strength of the horn vary along its longitudinal direction and show a distinct sensitivity on the strain rate.



## Chapter 4 Concluding Remarks

Despite the importance of the design of roadside safety hardware, most improvements are incremental and the past decade saw no significant changes. In sharp contrast, automobiles have evolved significantly over the years with the most notable example the wide adoption of electric vehicles. Innovative designs of roadside safety hardware are urgently needed to improve the level of safety and decrease the severity of accidents. In nature, many plants and animals are optimized to adapt to various overload conditions and have demonstrated superior impact-resistant and energy-absorbing capabilities, including tree bark, coconut endocarp, sea urchin spines, and bovid horns. The tree bark demonstrates an impressive damping capability due to its fibrous nature and multi-layered hierarchical structure; the coconut endocarp uses crack deflection, crack branching, and crack trapping as strengthening and toughening mechanisms of impact protection; the sea urchin spines possess a very high initial crushing strength and significant energy dissipation via graceful-failure fracture behavior, mainly thanks to its porosity variation; the bovid horn exhibits superior energy-absorbing and load-bearing capacities, mainly attributed to its curved conical shape, core-shell structure, and variations in the mechanical properties along its length direction. Careful examination of these biological structures may inspire a new generation of roadside safety structural designs. The strategies used by the biological role models can be understood, abstracted, modified, and transferred to bio-inspired roadside safety hardware.

## References

- [1] NHTSA, "Traffic Safety Facts 2015," National Highway Traffic Safety Administration, U.S. Department of Transportation, 2017.
- [2] Savolainen P.T., Barnwal A., Kirsch T.J., "Crash Cushion Selection Criteria, Final Report to the Iowa Department of Transportation," Iowa State University Center for Transportation Research and Education, Ames, Iowa, September 2017.
- [3] AASHTO, "Roadside Design Guide," American Association of State Highway and Transportation Officials, Washington, D.C., 2011.
- [4] NCHRP, "NCHRP Report 350, Recommended Procedures for the Safety Performance," Transportation Research Board, National Research Council, Washington, D.C., 1993.
- [5] AASHTO, "Manual for Assessing Safety Hardware," American Association of State Highway and Transportation Officials, Washington, D.C., 2009.
- [6] CEN, "EN 1317 Road Restraint Systems," European Committee for Standardization, Brussels, 2010.
- [7] Office of Safety, "Roadside Safety Hardware Identification Methods," Federal Highway Administration, U.S. Department of Transportation, 11 08 2020. [Online]. Available: [https://safety.fhwa.dot.gov/roadway\\_dept/countermeasures/reduce\\_crash\\_severity/id\\_methods/ch1.cfm#ss1](https://safety.fhwa.dot.gov/roadway_dept/countermeasures/reduce_crash_severity/id_methods/ch1.cfm#ss1). [Accessed 08 08 2021].
- [8] FDOT, "Bridge Maintenance Course Series," Bridge Division, Florida Department of Transportation, Tallahassee, Florida, 2018.
- [9] [Online]. Available: <http://www.ingalcivil.com.au/products/road-safety-barriers/wire-rope-safety-barrier/mashflex---mash-tl3-wrsb>. [Accessed 08 08 2021].
- [10] [Online]. Available: <http://www.csppacific.co.nz/news-item/new-mash-sentry-barrier-systems-from-csp>. [Accessed 08 08 2021].
- [11] [Online]. Available: <http://debonte.com/en/products/rebloc-safety-barriers/>. [Accessed 08 08 2021].
- [12] [Online]. Available: [http://www.abovebeyondconcepts.com.au/client\\_images/1646719.pdf](http://www.abovebeyondconcepts.com.au/client_images/1646719.pdf). [Accessed 08 08 2021].

- [13] Alberson D.C., Buth C.E., Menges W.L., Haug R.R., "NCHRP Report 350 Testing and Evaluation of NETC Bridge Rail Transitions," Texas Transportation Institute, College Station, Texas, January 2006.
- [14] Miller K. and Levin A., "NTSB 'unhappy' Tesla disclosed details of fatal crash," *Automotive News*, 01 04 2018. [Online]. Available: <http://www.autonews.com/article/20180401/OEM11/304019988/ntsb-unhappy-tesla-disclosed-details-of-fatal-crash>. [Accessed 08 08 2021].
- [15] [Online]. Available: <http://trinityhighway.com/product/energite-iii>. [Accessed 08 08 2021].
- [16] [Online]. Available: <http://www.valmonthighway.com/products-solutions/crash-cushions/raptor>. [Accessed 08 08 2021].
- [17] [Online]. Available: <http://www.enterpriseflasher.com/prod-permanent-easi-cell.php>. [Accessed 08 08 2021].
- [18] [Online]. Available: <http://www.acprod.com.au/products/universal-tauiii-crash-cushion>. [Accessed 08 08 2021].
- [19] [Online]. Available: <http://trinityhighway.com/product/adiem/>. [Accessed 08 08 2021].
- [20] Gabler H.C., "The risk of fatality in motorcycle crashes with roadside barriers," in *Proceedings of the Twentieth International Conference on Enhanced Safety of Vehicles*, Lyons, France, 2007.
- [21] MacDonald M.D., "Motorcyclists and roadside safety hardware," in *A2A04 Summer Meeting*, Pacific Grove, California, USA, 2002.
- [22] NPRA, "MC Safety Design and Operation of Roads and Traffic Systems," Directorate of Public Roads, Norwegian Public Roads Administration, Norway, 2004.
- [23] Daniello A. and Gabler H.C., "Effect of barrier type on injury severity in motorcycle-to-barrier collisions in North Carolina, Texas, and New Jersey," *Transportation Research Record: Journal of the Transportation Research Board*, vol. 2262, no. 1, pp. 144-151, 2011.
- [24] Moradi R., Ramamurthy S., Thorbole C.K., Bhonge P.S., Lankarani H.M., "Kinematic analysis of a motorcyclist impact on concrete barriers under different road conditions," in *Proceedings of the ASME 2010 International Mechanical Engineering Congress & Exposition*, Vancouver, British Columbia, Canada, 2010.

- [25] Grzebieta R., Bambach M., McIntosh A., "Motorcyclist impacts into roadside barriers: Is the European crash test standard comprehensive enough?," *Transportation Research Record: Journal of the Transportation Research Board*, vol. 2377, pp. 84-91, 2013.
- [26] IEA, "Report: Global EV Outlook 2021-Accelerating ambitions despite the pandemic," International Energy Agency, 2021.
- [27] IEA, "Report: Global EV Outlook 2017-Two Million and Counting," International Energy Agency, 2017.
- [28] Ehrensperger A., "E-crash – electric traffic," AXA Newsroom, 22 08 2019. [Online]. Available: <http://www.axa.ch/en/privatkunden/blog/out-and-about/security-on-the-road/crash-test-electric-car.html>. [Accessed 08 08 2021].
- [29] Jørgensen J.S., "EVs involved in far more accidents than conventional cars," RITZAU, 27 01 2020. [Online]. Available: <http://energywatch.eu/EnergyNews/Cleantech/article11900882.ece>. [Accessed 08 08 2021].
- [30] Tesla Team, "There is no “unintended acceleration” in Tesla vehicles," Tesla, 20 01 2020. [Online]. Available: <http://www.tesla.com/blog/no-unintended-acceleration-tesla-vehicles>. [Accessed 08 08 2021].
- [31] Noel S.R., "Will electric cars result in quieter communities?," Harris Miller Miller & Hanson Inc. , 15 04 2021. [Online]. Available: <http://hmmh.com/resources/news-insights/blog/will-electric-cars-result-in-quieter-communities>. [Accessed 08 08 2021].
- [32] Valdes-Dapena P., "Why electric cars are so much heavier than regular cars?," CNN Business, 07 06 2021. [Online]. Available: <http://www.cnn.com/2021/06/07/business/electric-vehicles-weight/index.html>. [Accessed 08 08 2021].
- [33] Krisher T., "Tesla Model S hits road debris and catches fire in Tennessee," Associated Press, 07 11 2013. [Online]. Available: <http://www.therecord.com/business/2013/11/07/tesla-model-s-hits-road-debris-and-catches-fire-in-tennessee-3rd-fire-in-company-s-electric-car.html>. [Accessed 08 08 2021].
- [34] Stokes A., Salin F., Kokutse A., Berthier S., Jeannin H., Mochan S., Dorren L., Kokutse N., Abd. Ghani M., Fourcaud, T., "Mechanical resistance of different tree species to rockfall in the French Alps," *Plant and Soil*, vol. 278, pp. 107-117, 2005.
- [35] Bold G., Langer M., Bornert L., Speck T., "The protective role of bark and bark fibers of the Giant Sequoia (*Sequoiadendron giganteum*) during high-energy impacts," *Int. J. Mol. Sci.*, vol. 21, no. 9, p. 3355, 2020.

- [36] Schmier S., Hosoda N., Speck T., "Hierarchical structure of the *Cocos nucifera* (coconut) endocarp: functional morphology and its influence on fracture toughness," *Molecules*, vol. 25, no. 1, p. 223, 2020.
- [37] Schmier S., Jentsch M., Speck T., Thielen M., "Fracture mechanics of the endocarp of *Cocos nucifera*," *Materials & Design*, vol. 195, p. 108944, 2020.
- [38] Presser V., Schultheiß S., Berthold C., Nickel K.G., "Sea Urchin Spines as a Model-System for Permeable, Light-Weight Ceramics with Graceful Failure Behavior. Part I. Mechanical Behavior of Sea Urchin Spines under Compression," *Journal of Bionic Engineering*, vol. 6, no. 3, p. 203, 2009.
- [39] Li B.-W., Zhao H.-P., Feng X.-Q., "Static and dynamic mechanical properties of cattle horns," *Materials Science and Engineering: C*, vol. 31, no. 2, p. 179, 2011.